

1 **The rapid deglaciation of the Skagafjörður fjord, northern Iceland**

2 NURIA ANDRÉS, DAVID PALACIOS, ÞORSTEINN SÆMUNDSSON, SKAFTI
3 BRYNJÓLFSSON, AND JOSÉ M. FERNÁNDEZ-FERNÁNDEZ

4 Andrés, N., Palacios, D., Sæmundsson, Þ., Brynjólfsson, S., and Fernández-Fernández,
5 J.M.: The rapid deglaciation of the Skagafjörður fjord (north Iceland).

6 The Skagafjörður fjord in northern Iceland is located between the Tröllaskagi Peninsula in
7 the east and the Skagi Peninsula in the west. The tributary valleys of the fjord originate in
8 the highland area about 15 km north of the Hofsjökull icecap. The results of this work
9 improve the knowledge of the deglaciation pattern in Skagafjörður and explore the
10 adequacy of the ³⁶Cl cosmic ray exposure dating method in an Icelandic environment, where
11 this method has rarely been applied to deglaciated surfaces. The ³⁶Cl dating method was
12 applied to 13 rock samples taken on a transect from the coastal areas towards the highlands.
13 All samples were obtained from rock outcrops with glacier-polished surfaces from the Last
14 Glaciation and from one of the few well-preserved erratic boulders. The cosmogenic
15 results, combined with previous radiocarbon results, indicate that the ice margin was
16 situated in the outermost sector of Skagafjörður at approximately 17–15 ka BP.
17 Subsequently, it retreated and occupied the central part of the fjord between 15 and 12 ka
18 BP and then the innermost sector of the fjord about 11 ka BP. The samples collected
19 between this position and the highlands show an average age of approximately 11 ka,
20 indicating rapid deglaciation after the early Preboreal. These results agree with earlier
21 studies of the deglaciation history of northern Iceland, reinforce previous deglaciation
22 models in the area and enable a better understanding of glacial evolution in the North
23 Atlantic from the Late Pleistocene to Holocene transition.

24 Keywords: Deglaciation, Tröllaskagi Peninsula, Cosmogenic Radionuclide Exposure
25 dating, ³⁶Cl Isotope, Iceland.

26 Abbreviations: IIS: Icelandic Ice Sheet, LGM: Last Glacial Maximum, LIA: Little Ice Age,
27 HTM: Holocene Thermal Maximum, CRE: Cosmic-Ray Exposure.

28 *Nuria Andrés (nandresp@ucm.es) High Mountain Physical Geography Research Group.*
29 *Department of Geography, Complutense University of Madrid, 28040 Madrid, Spain.*
30 *David Palacios, High Mountain Physical Geography Research Group. Department of*
31 *Geography, Complutense University of Madrid, 28040 Madrid, Spain. Þorsteinn*
32 *Sæmundsson, Faculty of Life and Environmental Science, University of Iceland, Öskju,*
33 *Sturlugötu 7, 101 Reykjavík, Iceland. Skafti Brynjólfsson, Icelandic Institute of Natural*
34 *History, Borgum vid Norðurslóð, Box 180, 602 Akureyri, Iceland. José M. Fernández-*
35 *Fernández, High Mountain Physical Geography Research Group. Department of*
36 *Geography, Complutense University of Madrid, 28040 Madrid, Spain.*

37
38

39

40

41 The deglaciation of the Northern Hemisphere ice sheets is considered the primary cause of
42 changes in sea surface temperature and salinity in the North Atlantic and of planetary
43 climate change, due to its influence on the Atlantic meridional overturning circulation
44 during the Late Pleistocene and Holocene (Clark *et al.* 2012; Renssen *et al.* 2012; Chen *et*
45 *al.* 2015; Gil *et al.* 2015; Jaccard *et al.* 2016; Lippold *et al.* 2016; Xiao *et al.* 2017). The
46 evolution of palaeo-ice sheets is increasingly attracting attention to interpret the changes
47 observed in modern ice sheets in the Northern Hemisphere and their contribution to sea-
48 level rise (Clark *et al.* 2009; Carlson & Clark 2012; Kleman & Applegate 2014; Stokes *et*
49 *al.* 2015; Hughes *et al.* 2016; Liakka *et al.* 2016; Sinclair *et al.* 2016; Stroeven *et al.* 2016;
50 Stokes, 2017). In this context, knowledge of the temporal evolution of the Icelandic ice
51 sheet (IIS) is of particular importance to understand the climatic interconnections between
52 the Greenland and Eurasian ice sheets and the potential spatio-temporal variability across
53 the northern North Atlantic. The position of Iceland is particularly important due to the
54 meeting of the northward-flowing North Icelandic Irminger Current and the southward-
55 flowing Arctic East Greenland Current (Malmberg 1985). These factors make the Icelandic
56 glaciers and environment extremely vulnerable and sensitive to any change in ocean
57 circulation patterns (Andrews & Giraude 2003; Xiao *et al.* 2017).

58 The IIS covered the whole island during the Last Glacial Maximum (LGM). The ice was
59 approximately 2 km thick at its centre (Hubbard *et al.* 2006) and the grounded ice reached
60 the shelf edge, about 150 km off the present coastline of north Iceland, between 29.1 and
61 18.6 cal. ky BP according to radiocarbon ages of submarine glaciogenic sediment cores
62 (Andrews *et al.* 2000; Spagnolo & Clark 2009; see synthesis and discussion in Pétursson *et*
63 *al.* 2015 and Patton *et al.* 2017). Approximately 18.6 cal. ky BP, the sea level started to rise
64 around Iceland (Andrews *et al.* 2000; Ingólfsson & Norðdahl 2001). During the Bølling
65 interstadial (14.7 to 14.1 ka BP), the IIS retreated rapidly, or rather collapsed, because of
66 significant sea-level rise (Norðdahl & Ingólfsson 2015). During this time, the IIS covered
67 the centre and southeast of the island (Norðdahl & Ingólfsson 2015; Pétursson *et al.* 2015).
68 Changes in pollen, marine sediments and sea levels suggest a cold period and glacial
69 advances at the end of the Bølling interstadial, around 14 cal. ka BP according to

70 radiocarbon dates ([Ingólfsson et al. 1997](#); [Pétursson et al. 2015](#) Changes in pollen and
71 radiocarbon dates collected in Lake Torfadalsvatn on the Skagi Peninsula demonstrated that
72 shrub tundra vegetation was established in the Peninsula, with temperatures rising almost to
73 present levels during the Allerød interstadial (13.9 to 12.9 ka BP; [Rundgren 1995, 1999](#);
74 [Rundgren & Ingólfsson 1999](#)).

75 The Younger Dryas stadial (12.9 to 11.7 ka BP) is reflected in Iceland by the clear IIS re-
76 advance. In northern Iceland, the glaciers expanded and reached the present coastline and
77 entered the fjords, but many interfluves remained ice-free during this period (see synthesis
78 in [Pétursson et al. 2015](#)). The sudden cooling at the beginning of the Younger Dryas is
79 demonstrated in the Skagi Peninsula in a change to grass tundra, which reverted to shrub
80 tundra vegetation at the end of this stadial, according to pollen records ([Rundgren 1995](#),
81 [1999](#)).

82 The IIS retreated at the end of the Younger Dryas and re-advanced again in the early
83 Preboreal, around 11.2 ka BP (see synthesis in [Pétursson et al. 2015](#)). During this period,
84 the IIS advanced into the fjords in northern Iceland ([Ingólfsson et al. 1997](#); [Norðdahl &](#)
85 [Einarsson 2001](#); [Norðdahl & Pétursson 2005](#)). After 11.2 ka BP the glaciers retreated
86 rapidly ([Kaldal & Víkingsson 1990](#); [Andrews et al. 2000](#); [Norðdahl & Einarsson 2001](#);
87 [Geirsdóttir et al. 2002, 2009](#)). By 10.3 ka BP, when the Saksunarvatn tephra was deposited,
88 much of the centre and north of Iceland was already deglaciated ([Stötter et al. 1999](#);
89 [Caseldine et al. 2003](#); [Larsen et al. 2012](#); [Striberger et al. 2012](#)). Research in the Vestfirðir
90 Peninsula, in the northwest of Iceland where, Drangajökull ice cup still remain, reports a
91 local icecap during the LGM, which remained during the whole deglaciation of this
92 Peninsula, with evidence derived from cosmogenic dating ([Principato et al. 2006](#)). About
93 when the Saksunarvatn tephra was deposited, the dimensions of this local icecap were
94 suggested to have been similar to its present dimensions, according to radiocarbon dating of
95 pollen and macrofossil plants covered by the Saksunarvatn tephra in some Vestfirðir
96 Peninsula lakes ([Eddudóttir et al. 2015, 2016](#); [Harning et al. 2016](#)). However, different
97 behaviour of Drangajökull and later deglaciation at southeast of Drangajökull have been
98 suggested, supported by ^{14}C and tephrochronology ages in lake sediment cores
99 ([Schomacker et al. 2016](#)). Recent work, supported by ^{14}C dates from entombed dead

100 vegetation and lake sediment records, disputes this partial contradiction and supports
101 deglaciation of the southeast part of Drangajökull during the Lateglacial or Early Holocene
102 (Harning et al. 2018). Furthermore, cosmogenic exposure dating of glacial landforms and
103 boulders in coastal areas around Drangajökull indicates that extensive outlet glaciers to the
104 north and northeast of the present Drangajökull icecap persisted at least until c. 9 ka BP
105 (Brynjólfsson et al. 2015). Despite our improved understanding of the deglaciation in
106 Iceland, several issues remain uncertain, for example the deglaciation pattern in the
107 northern part of the island, especially around the Tröllaskagi Peninsula.

108 The cosmic ray exposure (CRE) dating method has been applied successfully to study the
109 geochronological deglaciation pattern of European ice sheets and mountains (see synthesis
110 in Ivy-Ochs 2015; Vasskog et al. 2015; Chenet et al. 2016; Hughes et al. 2016; Stroeven et
111 al. 2016; Wirsig et al. 2016; Dede et al. 2017; Palacios et al. 2017b; Stokes 2017); however,
112 it is still rarely applied to improve deglaciated surface studies in Iceland (Principato et al.
113 2006; Brynjólfsson et al. 2015). This may be because quartz is absent in basalts, the most
114 prevalent rocks in Iceland, and the Be10 dating method cannot be applied; also, the
115 intensive erosion and weathering hinders finding original deglaciated surfaces and these
116 surfaces may occasionally have been covered by ash layers shielding them from cosmic
117 radiation. However, the ^{36}Cl dating method has been applied successfully in basalts
118 (Swanson & Caffee 2001; Phillips 2003; Principato et al. 2006; Licciardi et al. 2008;
119 Schimmelfennig 2009; Schimmelfennig et al. 2009, 2011; Brynjólfsson et al. 2015); the
120 CRE results can be validated by other methods previously applied, mainly radiocarbon
121 dating. Moreover, some well-preserved protruding glacial landforms can be observed in
122 Skagafjörður where ash was almost immediately blown away after recent eruptions, which
123 enables them to be targeted for CRE dating.

124 This study aimed to present a new data set of ^{36}Cl cosmogenic exposure dates to improve
125 our understanding of the deglaciation pattern in the Skagafjörður from during the
126 Lateglacial until the Holocene. Although ^{36}Cl production systematics are complex, the ^{36}Cl
127 production rate parameters have been improved recently (Schimmelfennig et al. 2009;
128 Marrero et al. 2016a, b). For these reasons, this work also aimed to explore the possibility

129 of obtaining an adequate geochronology of deglaciation in Iceland by applying the new ^{36}Cl
130 age models.

131 **Study Area**

132 *Location*

133 The Skagafjörður is located in central northern Iceland, between the Tröllaskagi Peninsula
134 to the east and the Skagi Peninsula to the west (Fig. 1). This U-shaped fjord is ~25 km wide
135 at the mouth and 12 km wide at the current coastline. The broad, flat valley bottom gently
136 narrows inland. About 30 km south of the present coastline, the valley continues up to the
137 highland plateau in three tributary valleys: Svartárdalur to the west, Vesturárdalur in the
138 centre and Austurdalur to the east (Fig. 1). These valleys cut into the highland plateau at
139 700–800 m a.s.l. north of the Hofsjökull icecap. To the west of Skagafjörður, a 700–1000
140 m high mountain chain continues from the highland plateau in the south towards the Skagi
141 Peninsula. To the east, a higher and broader mountain chain, the Tröllaskagi Peninsula,
142 separates the Skagafjörður and Eyjafjörður fjords. This mountain massif is up to 1500 m
143 high and 40–50 km wide with numerous tributary valleys. The Peninsula has been sculpted
144 by glacial erosion with glacially carved fjords, valleys and cirques, with over 150 alpine
145 glaciers at present (Sigurðsson & Williams 2008). The bedrock in the area dates to 16–3.3
146 Ma (Moorbath et al. 1968; Watkins & Walker 1977; McDougall et al. 1984) and is mostly
147 composed of jointed basaltic lava flows 2–30 m thick, often separated by lithified
148 sedimentary horizons 30–50 m thick (Sæmundsson 1979; Sæmundsson et al. 1980;
149 Hjartarson & Sæmundsson 2014). The upper parts of the valley slopes, at 600–900 m a.s.l.,
150 are often very steep, while the lower parts are gentler and generally covered by glacial
151 deposits or debris talus. The slopes are also affected by numerous rock slope failures and
152 deep-seated gravitational slope deformation, where the red interbed layers act as
153 decollement levels (Jónsson 1976; Cossart et al. 2014; Feuillet et al. 2014). These macro-
154 mass movements have been described as the paraglacial response of the deglaciation during
155 the Early Holocene (Mercier et al. 2013, 2017; Cossart et al. 2014; Coquin et al. 2015;
156 Decaulne et al. 2016), although in fact, some are still active (Wangensteen et al. 2006).

157 *Previous knowledge of the Skagafjörður deglaciation patterns*

158 During the Last Maximum Glaciation extent in Iceland, the north part of Skagafjörður was
159 covered by ice extending far beyond the present coastline, confirmed by radiocarbon dating
160 of glacial marine sediments (see synthesis in Pétursson et al. 2015 and Patton et al.
161 2017). The striation pattern in the Skagafjörður area indicates an ice-flow direction parallel
162 to the main fjord in a northward direction and a predominantly westward direction from the
163 main tributary valleys on the eastern side of the fjord (Víkingsson 1978; Bourgeois et al.
164 2000). Pollen, diatom and organic carbon analyses in the sedimentary series of the
165 Torfadalsvatn and other nearby lakes on the outermost part of the Skagi Peninsula
166 (Rundgren 1995; Rundgren & Ingólfsson 1999) have revealed that deglaciation was already
167 underway in the Allerød interstadial. Severe cooling occurred during the Younger Dryas,
168 with a significant impact on vegetation, but the Skagi Peninsula remained ice-free
169 (Rundgren 1995; Rundgren & Ingólfsson 1999). The Younger Dryas ice extent in
170 Skagafjörður is not well marked, except for radiocarbon-dated shells around 12 cal. ka BP
171 and for Vedde Ash distribution (12.1 cal. ka BP). From this information, some authors have
172 deduced the glacier margin to have been on the lowlands close to the present coastline
173 (Norðdahl & Pétursson 2005; Norðdahl et al. 2008), but others consider that the glacier
174 front extended a few km beyond the current coastline (Pétursson et al. 2015). It is not
175 known either where the Skagafjörður glacier was located during the Preboreal; however,
176 the glacier probably terminated on land, occupying the main valleys of Skagafjörður by
177 11.2 cal. ka BP, according to fossil marine molluscs, with a relative sea level at around 40–
178 50 m above the present level, when the Skagi Peninsula was free of ice as observed from
179 lake sediments (Ingólfsson et al. 1997; Norðdahl & Pétursson 2005). After the Preboreal,
180 the temperature rose during the first half of the Holocene (Caseldine et al. 2006; Geirsdóttir
181 et al. 2013). In fact, the expansion of birch in Tröllaskagi had begun by 10 ka BP, reaching
182 its maximum between 8 and 5 ka BP, that is during the Holocene Thermal Maximum
183 (Wastl et al. 2001; Caseldine et al. 2006).

184 **Material and methods**

185 Research into the deglaciation pattern in the Skagafjörður was approached through a
186 number of fieldwork campaigns during the summers of 2010, 2012, 2014 and 2015, using
187 fieldwork and photo-interpretation to identify the most suitable landforms for sampling

188 purposes, including glacially polished bedrock outcrops, moraines and erratic boulders. The
189 main tributary valleys on the eastern side of the Skagafjörður, namely Hjaltadalur,
190 Hóladalur, Kolbeinsdalur, Deildardalur and Unadalur (Fig. 1) were surveyed during four
191 summer periods, but no appropriate glacial landforms to apply CRE dating methods were
192 observed. No bedrock outcrops or outstanding blocks are evident in the relief of these
193 tributary valleys, with the exception of those generated by postglacial rock avalanches.
194 Sampling in Skagafjörður was carried out from the highlands to the north of the Hofsjökull
195 icecap to the coastal areas and that also extended along the fjord shoreline onto the Skagi
196 Peninsula, a total distance of 170 km (Figs 2, 3; Table 1). There are only 10 glacially
197 polished bedrock outcrops suitable for sampling along this transect (Fig. 2). A sample was
198 collected from each of these outcrops and another from an erratic boulder. This boulder was
199 practically the only one found that showed signs of not having been altered by postglacial
200 processes. Additional samples were collected from the Eyjafjörður to compare the
201 deglaciation pattern of the two valleys: one located in the innermost part of the fjord and
202 the other one approximately 30 km to the north from this position (Fig. 2). Samples were
203 collected using a hammer and chisel from above 90 m a.s.l., as no higher shorelines above
204 that altitude have been observed after deglaciation in the area (Pétursson et al. 2015), which
205 could have disturbed the reception of cosmic radiation by the sampled surfaces.

206 The ^{36}Cl cosmogenic nuclide dating method was selected as the bedrock consists
207 predominantly of basalt, and phenocrysts could not be identified in the samples. Laboratory
208 procedures for ^{36}Cl analysis of whole rock samples (Zreda et al. 1999; Phillips 2003) were
209 followed. Whole rock samples were crushed and pulverized using a roller grinder. The
210 samples were then sieved to separate the 150–850 μm fraction and leached in deionized
211 water and nitric acid (HNO_3) to remove atmospheric Cl. Next, the samples were dissolved
212 in a hot mixture of hydrofluoric (HF) and nitric acids, and silver nitrate (AgNO_3) was
213 added to the solution to precipitate silver chloride (AgCl). Sulphur was separated by adding
214 barium nitrate ($\text{Ba}(\text{NO}_3)_2$) and consequently precipitating barium sulphate (BaSO_4). A
215 spike of isotopically enriched ^{35}Cl was added during the dissolution process. This isotope
216 dilution mass spectrometry enabled the natural $^{35}\text{Cl}/^{37}\text{Cl}$ ratio that is fixed at 3.1 to be
217 changed and thus enabled the determination of the Cl concentration in the sample (Ivy-
218 Ochs et al. 2004; Desilets et al. 2006) and of the sample Cl content from isotope dilution

219 accelerator mass spectrometry (AMS) measurements. The AMS analysis of the $^{36}\text{Cl}/^{35}\text{Cl}$
220 and $^{37}\text{Cl}/^{35}\text{Cl}$ ratios in the AgCl targets was carried out at the PRIME Laboratory (Purdue
221 University, USA). Aliquots of rock were analysed for major elements and trace elements at
222 the Activation Laboratories (Ancaster, Canada). These analyses were necessary to calculate
223 the relative contributions from the different composition-dependent ^{36}Cl production
224 pathways (Schimmelpfennig et al. 2009).

225 The exposure ages were calculated using the spreadsheet for *in-situ* ^{36}Cl exposure age
226 calculations proposed by Schimmelpfennig (2009) and Schimmelpfennig *et al.* (2009). We
227 used the cosmogenic ^{36}Cl production rates for Ca spallation by Stone *et al.* (1996) ($48.8 \pm$
228 3.4 atoms ^{36}Cl (g Ca) $^{-1}$ yr $^{-1}$), but we also used a production rate of 57.3 ± 5.2 atoms ^{36}Cl (g
229 Ca) $^{-1}$ yr $^{-1}$ (Licciardi *et al.* 2008); for K spallation by Schimmelpfennig *et al.* (2014) (148.1
230 ± 7.8 atoms ^{36}Cl (g K) $^{-1}$ yr $^{-1}$); for Ti spallation by Fink *et al.* (2000) (13 ± 3 atoms ^{36}Cl (g
231 Ti) $^{-1}$ yr $^{-1}$); and for Fe spallation by Stone *et al.* (2005) (1.9 atoms ^{36}Cl (g Fe) $^{-1}$ yr $^{-1}$). Finally,
232 we also applied the epithermal neutron production rate from fast neutrons in the atmosphere
233 at the land/atmosphere interface by Marrero *et al.* (2016b) (695 ± 185 neutrons (g air) $^{-1}$ yr $^{-1}$).
234

235 The *in-situ* accumulation of ^{36}Cl depends also on various factors including latitude,
236 elevation, sample thickness, surrounding topography and snow cover. The elevation-
237 latitude scaling factors for nucleonic and muonic production were evaluated using the time-
238 invariant “St” model of Stone (2000). The topographic shielding factor was calculated
239 using the Topographic Shielding Calculator v1.0 of CRONUS-Earth Project (2015).

240 The results obtained from the Schimmelpfennig et al. (2009) spreadsheet allowed us to
241 change the Ca spallation production rate according to either that of Stone et al. (1996),
242 derived from feldspar phenocrysts isolated from basaltic calibration samples, or Licciardi et
243 al. (2008), derived from basaltic whole rock calibration samples. The comparison of the
244 results from the two production rates are compared in Table 2. In both production rates, the
245 composition of the calibration samples was dominated by Ca (Stone et al. 1996; Licciardi et
246 al. 2008). The calibration sites of the Licciardi et al. (2008) production rate are located in
247 southwestern Iceland (see also Licciardi et al. 2006), permanently affected by a low
248 pressure cell (the ‘Icelandic Low’). For this reason, Licciardi et al.’s production rate already

249 accounts for this anomaly. Stone et al.'s production rate was calibrated in Tabernacle Hill
250 (Utah, central-western United States) and hence needs to be corrected to be applied in
251 Iceland.

252 **Results**

253 In total, 13 samples were collected on a north-south transect from the Hofsjökull ice-cap
254 north to the Skagi peninsula. The ages obtained from these 13 samples using the proposed
255 method range from 15.9 ± 1.2 ka to 6.8 ± 0.5 ka as shown in Table 2 and Figures 2 and 3.

256 Two samples, SK-2 located 146 km (137 m a.s.l.) and SK-3 located 161 km (95 m a.s.l.)
257 north of the Hofsjökull icecap, were collected from polished ridges on the Skagi Peninsula
258 and yielded ages of 15.9 ± 1.2 and 15.8 ± 1.1 ka, respectively (Figs 2, 3). Sample IF-9 was
259 collected from a polished surface on the summit of the Þórðarhöfði cape, located on the
260 eastern side of the Skagafjörður, approximately 104 km north of the Hofsjökull icecap, and
261 yielded an age of 12.7 ± 0.9 ka (Figs 2, 3, 4). On the opposite side of the fjord, sample SK-
262 1 was collected from a polished ridge, approximately 132 km and 162 m a.s.l., north of the
263 Hofsjökull icecap, yielding an age of 11.9 ± 0.9 ka.

264 Sample IF-8 was collected from an ice-polished ridge at 129 m a.s.l., by the present
265 shoreline of the Skagafjörður fjord, approximately 92 km north of the Hofsjökull icecap,
266 and yielded an age of 10.7 ± 0.7 ka (Figs 2, 3).

267

268 Two other samples (IF-6 and IF-7) were collected from a polished lowland ridge at the
269 bottom of the valley, approximately 90 km north of the Hofsjökull icecap at 139 and 122 m
270 a.s.l., respectively. Sample IF-6 was collected on the top of the ridge and yielded an age
271 (10.6 ± 0.7 ka) similar to IF-2 and IF-3. Sample IF-7, collected approximately 20 m below
272 the IF-6 site, yielded a younger age (9.2 ± 0.6 ka) (Figs 2, 3, 5).

273 Two other samples (IF-4 and IF-5) were collected on a polished ridge at 150 m a.s.l., which
274 divides the Vesturárdalur valley longitudinally, approximately 70 km north of the
275 Hofsjökull icecap. These samples yielded ages of 9.6 ± 0.7 and 6.8 ± 0.5 ka, respectively
276 (Figs 2, 3). The southernmost sample in the series (IF-2) was collected from an erratic

277 boulder located 26 km from the Hofsjökull icecap at 704 m a.s.l., which yielded an age of
278 10.9 ± 0.7 ka (Figs 2, 3, 6). Approximately 10 km to the north, at 645 m a.s.l., a sample (IF-
279 3) was collected from a glacially polished bedrock outcrop, yielding a similar age ($10.4 \pm$
280 0.7 ka) to IF-2 (Figs 2, 3).

281 Two more samples were collected in the Eyjafjarðardalur valley. Sample AKU-1, collected
282 from a polished ridge at the mouth of this valley (~96 km north of the Hofsjökull icecap
283 and 202 m a.s.l.), yielded an age of 10.8 ± 0.7 ka (Figs 2, 3B). Sample AKU-2, also
284 collected from a polished ridge 30 km further north in the Eyjafjörður fjord and 210 m a.s.l.
285 (Fig. 2), yielded an age of 15.3 ± 1.0 ka (Fig. 7).

286 **Discussion**

287 Various glacial landforms, especially moraines, have been mapped and related to the
288 deglaciation history of Iceland. However, only a few of these landforms have been dated,
289 mainly due to the lack of organic material for radiocarbon dating, especially in northern
290 Iceland (Kaldal & Víkingsson 1990; Norðdahl & Pétursson 2005; Norðdahl et al. 2008).
291 The lake records are the most reliable, as they capture continuous sedimentation during
292 deglaciation, and the boundary between glacial and non-glacial sediment can be dated by
293 both radiocarbon and tephrochronology (Rundgren 1995; Rundgren & Ingólfsson 1999;
294 Larsen et al. 2012; Striberger et al. 2012; Harning et al. 2016, 2018; Schomacker et al.
295 2016). ^{36}Cl CRE dating methodology has rarely been applied in Iceland to deglaciated
296 surfaces (Principato et al. 2006; Brynjólfsson et al. 2015). Therefore, the possible
297 application of the ^{36}Cl CRE dating method to reconstruct the deglaciation history of the
298 Skagafjörður fjord and contrast with lake records from surrounding areas opens up new
299 perspectives in our understanding of this deglaciation.

300 During the Skagafjörður sampling, it was difficult to find landforms meeting the
301 appropriate sampling criteria as many of the slopes and the bottom of the fjord are covered
302 by soils, tephra and other sediments, which shield the glacial surfaces from cosmic
303 radiation and thus disturb the ^{36}Cl surface production. In addition, much of the area has
304 been affected by landslides, solifluction or floods, which has led to the destruction of
305 glacial surfaces. No clear moraine formations have been observed, and practically all the

306 protruding outcrops that conserve glacier polishing were sampled. Taking these
307 circumstances into account, the only way to analyse the reliability of the results is to
308 observe their geomorphological location within the sampled transect, from the highlands to
309 the outermost part of the fjord.

310 The results obtained in most of the samples are properly sorted according to the
311 geomorphological logic, with the younger ones being closer to the current glacier front. Our
312 results obtained on the outermost part of the Skagi Peninsula (SK-2 and SK-3) suggest that
313 it was deglaciated after 17 ka. Previous ages obtained by radiocarbon dating in marine
314 sediments confirm that the glacier had retreated to the mid-shelf before 18.5 cal. ka BP
315 (Andrews et al. 2000). Radiocarbon dates in a nearby lake (Rundgren 1995; Rundgren &
316 Ingólfsson 1999) also demonstrated that the mouth of the fjord was deglaciated by 15 ka.
317 The radiocarbon and cosmogenic ages suggest that the IIS limit was most likely situated at
318 the mouth of the Skagafjörður, before 17–15 ka BP, following the rapid rise in sea level
319 from c. 18.6 ka BP (Andrews et al. 2000). Previous data from northern Iceland, based on
320 criteria of radiocarbon-dated lacustrine and littoral sediments and tephrochronology dating,
321 also support this ice-margin location (Kaldal & Víkingsson 1990; Eiríksson et al. 2000;
322 Norðdahl & Einarsson 2001; Norðdahl et al. 2008). Nevertheless, the limited number of
323 samples and the wide range of uncertainty obtained in this work do not allow the exact
324 location of the ice margin to be defined. The 17–15 ka BP period is coincident with the
325 Oldest Dryas (stadial GS-2a, between 17.5 and 15 ka BP). There are no existing references
326 that can clarify the potential impact of cooling on the Icelandic glaciers in this period, but
327 an overall trend of continental deglaciation following the end of the LGM was abruptly
328 interrupted in many parts of Europe during the Oldest Dryas (Eiríksson et al. 2000; Ivy-
329 Ochs 2015; Palacios et al. 2017a). During this period, there was a significant reduction in
330 the meridional overturning circulation (McManus et al. 2004). In addition to these climatic
331 proxies, other factors must be taken into account in stabilizing the ice sheet between 17 and
332 15 ka BP, such as topography and the role that the coastline at that time may have played in
333 its stabilization, as happened with other ice sheets (Stokes et al. 2014). In fact, several
334 studies have suggested an IIS stepwise retreat (see review in Geirsdóttir et al. 2009), and
335 recent work in the Vestfirðir Peninsula in northwest Iceland also demonstrates that the IIS
336 response to climatic forcing is not linear (Brynjólfsson et al. 2015). Patton et al. (2017)

337 relate the IIS retreat patterns in the north not only to the climate evolution but also to basal
338 topography and sea-level changes.

339 The destabilization of the IIS itself, due to a rapid sea-level rise, may have caused its
340 collapse with a rapid retreat just around 15 ka (see synthesis in Norðdahl & Ingólfsson
341 2015; Pétursson et al. 2015; Patton et al. 2017). Ingólfsson & Norðdahl (2001) first
342 suggested that this global sea-level rise was caused by the intensive melting of the northern
343 ice sheets and provoked massive calving in the IIS and its collapse. Our two samples
344 located further to the south on each side of the fjord about 130 km from the Hofsjökull
345 icecap (IF-9 and SK-1) give 12.7 ± 0.9 and 11.9 ± 0.9 ka, respectively. These ages would
346 place the retreat of the ice margin from the central part of the fjord around 15–11.5 ka BP
347 and support a rapid and intensive retreat after 15 ka BP (around 25 km), but once again, the
348 small number of samples and the range of uncertainty do not give us the exact location of
349 the ice margin. These ages are also coincident with the deglaciation of the Torfadalsvatn
350 dated by radiocarbon and the expansion of shrub tundra vegetation in the Skagi Peninsula
351 according to pollen collected in the lake sediments between 13.9 and 12.9 ka BP, with
352 bioclimatic conditions similar to the present (Rundgren 1995, 1999; Rundgren &
353 Ingólfsson 1999). Extensive subaerial lava flows to the east of Tröllaskagi confirm the large
354 deglaciation areas in the north of Iceland during this period (Norðdahl & Pétursson 2005).
355 Norðdahl et al. (2008) and Pétursson et al. (2015) modelled the glacier limit during the
356 Allerød interstadial and during the Younger Dryas maximum in Skagafjörður, following
357 the radiocarbon ages, mollusc fauna and the shoreline distribution criteria. According to
358 these models, the SK-1 and IF-9 samples are within the Bølling deglaciation areas but just
359 outside of the Younger Dryas advance. A similar situation for our samples is obtained from
360 the more complex numerical model proposed by Patton et al. (2017) (Fig. 2).

361 The results of our samples do not allow us to define the position of the ice margin in
362 Skagafjörður during the Younger Dryas period that led to major biosphere degradation in
363 the north of Iceland (Rundgren 1995, 1999) and sea-ice conditions (Xiao et al. 2017).
364 Previous publications have demonstrated that the glaciers reoccupied valleys and reinvaded
365 the fjords to their middle sector during this period in northern Iceland, leaving terminal
366 moraines on the bottoms, according to shoreline distribution radiocarbon dating (Pétursson

367 et al. 2015). The very few radiocarbon and tephrochronology dates that exist at present
368 along the shores of northern Iceland fjords show that they were already ice-free at the end
369 of the Younger Dryas period (Norðdahl & Haflidason 1992; Ingólfsson et al. 1997;
370 Eiríksson et al. 2000; Pétursson et al. 2015).

371 The ages of samples IF-2 (10.9 ± 0.7 ka), IF-3 (10.4 ± 0.7 ka), IF-4 (9.6 ± 0.7 ka), IF-6
372 (10.6 ± 0.7 ka), IF-7 (9.2 ± 0.6 ka) and IF-8 (10.7 ± 0.7 ka) are all statistically the same
373 considering their range of uncertainty (Figs 2, 3, 5, 8). Anomalously, the age of IF-5 ($6.8 \pm$
374 0.5 ka) is younger than the samples collected closer to the present glacier. We consider the
375 sample IF-5 an outlier, which could be explained by previous burial. The other six samples
376 located between the present shoreline and the Hofsjökull icecap (IF-2, IF-3, IF-4, IF-6, IF-7
377 and IF-8) all give similar ages and show an arithmetic mean of 10.2 ka. The absence of the
378 Skogar-Vedde Tephra, dated to 12.1 cal. ka BP, and the presence of the Saksunarvatn
379 tephra, dated to 10.3 cal. ka BP (Stötter et al. 1999; Caseldine et al. 2006; Rasmussen et al.
380 2006), suggest that this area was most probably deglaciated after ~ 12.1 ka and before ~ 10.3
381 ka. Further evidence based on truncated raised shorelines and radiocarbon dating suggests
382 that during the early Preboreal, a new re-advance occurred in northern Iceland during which
383 the glacier margins advanced into the fjords (Ingólfsson et al. 1997; Norðdahl & Einarsson
384 2001; Norðdahl & Pétursson 2005; Pétursson et al. 2015). The results obtained for the age
385 distribution of our samples between the ages of two well-known tephra deposits inland
386 from the present coastline agree with early Preboreal truncated raised shorelines and
387 radiocarbon dating (Ingólfsson et al. 1997). According to this information, the ice margin in
388 Skagafjörður was located not far inland from the present shoreline during the early
389 Preboreal period, when the Skagi Peninsula was mostly ice-free (Figs 1, 2).

390 The similar ages of the six samples, with an average of c. 10.2 ka, and the previous criteria,
391 suggest abrupt deglaciation at the end of the early Preboreal period, of more than 90 km of
392 glacier retreat in 1000 years, which is supported by previous deglaciation research in
393 Iceland (Kaldal & Víkingsson 1990; Andrews et al. 2000; Norðdahl & Einarsson 2001;
394 Geirsdóttir et al. 2002, 2009; Larsen et al. 2012; Pétursson et al. 2015). This rapid
395 deglaciation process after the Preboreal agrees with the latest models developed of
396 deglaciation in northern Iceland (Pétursson et al. 2015) (Fig. 2). Recently, similar results

397 have been obtained from the study of the deglaciation of Drangajökull, in northwest
398 Iceland, where radiocarbon dating of lake sediments demonstrates a rapid deglaciation of
399 the north side of this icecap in the Early Holocene, reaching its present extent at 10.3 cal. ka
400 BP (Harning et al. 2016).

401 It is possible that, in a complex glacier fluctuation scenario, there might be inherited ^{36}Cl
402 on glacially polished bedrock outcrops, where a glacial advance may not eliminate the
403 cosmogenic heritage accumulated previously. However, the chronological order of the
404 samples most distant from those closest to the current glacier front is respected. In addition,
405 the clustering of the ages of samples within the logical period limited by tephrochronology
406 and by the radiocarbon dating of the lakes and littoral sediments appears to defend the idea
407 of a lack of or limited cosmogenic inheritance in our samples.

408 The preliminary results from the only two samples in the Eyjafjörður agree with previous
409 research on the deglaciation of this fjord. The obstruction of the Fnjóskadalur valley,
410 tributary of the Eyjafjörður, started at 17 ka BP and ended by 12 ka BP, and it is estimated
411 that the glacier margin was located at the head of the Eyjafjörður at 11 ka BP (Einarsson
412 1967, 1973; Norðdahl 1991). The samples AKU-2 (15.3 ± 1.0) and AKU-1 (10.8 ± 0.7 ka)
413 are located in Eyjafjörður, on the opposite side of the mouth of the Fnjóskadalur and at the
414 head of the fjord, respectively (Fig. 2). The results of these exploratory samples support the
415 application of ^{36}Cl CRE methods in future research in Eyjafjörður.

416 **Conclusions**

417 The results of this work improve the knowledge of the glacial evolution of the Skagafjörður
418 in northern Iceland by applying cosmogenic dating methods. The results agree with
419 previous research based on other dating methods and with indicators of other
420 palaeoclimatic proxies. The ages of samples SK-2 and SK-3, complemented with
421 radiocarbon ages in lakes and marine sediments, suggest that the ice margin of the IIS was
422 located at the outermost parts of the Skagafjörður at approximately 17 ka BP. The samples
423 IF-8, IF-7, radiocarbon ages in lakes and littoral sediments and shoreline distribution
424 confirm the effects of glacial collapse around 15 ka BP in Skagafjörður. Similar ages from
425 six samples along a 70-km transect, together with tephrochronology and radiocarbon dating

426 of lake sediments and truncated shoreline distribution, suggest that the ice margin was
427 situated at the present coastline approximately at 11 ka BP and then retreated rapidly after
428 the Preboreal period. Between approximately 11 and 10 ka BP, the glacier retreated
429 proximal to the current margin of the Hofsjökull icecap in the central highland. These
430 results agree with previous studies of the deglaciation history of northern Iceland and
431 demonstrate the potential of the CRE dating method using ^{36}Cl to improve and define the
432 glacial history of Iceland. The lack of contradictions between the methods applied in
433 previous studies and the present study reinforces the models proposed previously. The
434 inherent limitation in the lack of well-preserved glacial landforms, a characteristic feature
435 of the Tröllaskagi Peninsula, should not discourage the application of CRE dating; on the
436 contrary, an adequate sampling strategy based on geomorphological criteria and exhaustive
437 fieldwork should offset this limitation.

438 **Acknowledgements**

439 This paper was supported by the project CGL2015-65813-R (Spanish Ministry of Economy
440 and Competitiveness) and Nils Mobility Program (EEA GRANTS) and with the help of the
441 High Mountain Physical Geography Research Group (Complutense University of Madrid).
442 We thank the Icelandic Institute of Natural History and the Hólar University College for
443 their support in the field. The authors express their deep gratitude to the two anonymous
444 reviewers whose detailed and interesting suggestions helped to improve our manuscript.
445 Advice and corrections by the Editor J.A. Piotrowski have been also of fundamental help to
446 improve the manuscript.

447 **References**

- 448 Andrews, J. T. & Giraude, J. 2003: Multi-proxy records showing significant Holocene
449 environmental. *Quaternary Science Reviews* 22, 175–193.
- 450 Andrews, J. T., Harðardóttir, J., Helgadóttir, G., Jennings, A.E., Geirsdóttir, Á.,
451 Sveinbjörnsdóttir, Á.E., Schoolfield, S., Kristjánisdóttir, G.B., Smith, L.M., Thors, K., &
452 Syvitski, J. 2000: The N and W Iceland Shelf: Insights into Last Glacial Maximum ice
453 extent and deglaciation based on acoustic stratigraphy and basal radiocarbon AMS dates.
454 *Quaternary Science Reviews* 19, 619-631.
- 455 Brynjólfsson, S., Schomacker, A., Ingólfsson, & Ó., Keiding, J.K. 2015: Cosmogenic ^{36}Cl
456 exposure ages reveal a 9.3 ka BP glacier advance and the Late Weichselian-Early Holocene

457 glacial history of the Drangajökull region, northwest Iceland. *Quaternary Science Reviews*
458 126, 140-157.

459 Bourgeois, O., Dauteuil, O., & van Vliet-Lanoë, B. 2000: Geothermal control on flow
460 patterns in the Last Glacial Maximum ice sheet of Iceland. *Earth Surface Processes and*
461 *Landforms* 25, 59-76.

462 Carlson, A.E. & Clark, P.U. 2012: Ice sheet sources of sea level rise and freshwater
463 discharge during the last deglaciation. *Reviews of Geophysics* 50, 1-72.

464 Caseldine, C., Geirsdottir, A., & Langdon, P. 2003: Efstadalsvatn—a multiproxy study of a
465 Holocene lacustrine sequence from NW Iceland. *Journal of Paleolimnology* 30, 55–73.

466 Caseldine, C., Langdon, P.G., & Holmes, N. 2006: Early Holocene climate variability and
467 the timing and extent of the Holocene Thermal Maximum (HTM) in northern Iceland.
468 *Quaternary Science Reviews* 25, 2314-2331.

469 Chen, T., Robinson, L.F., Burke, A., Southon, J., Spooner, P., Morris P. J., & Chin H.
470 2015: Synchronous centennial abrupt events in the ocean and atmosphere during the last
471 deglaciation. *Science* 25 349 (6255), 1537-1541.

472 Chenet, M., Brunstein, D., Jomeli, V., Roussel, E., Rinterknecht, V., Mokadem, F., Biette,
473 M., Robert, V., Leanni, L., & ASTER Team. 2016: ¹⁰Be cosmic-ray exposure dating of
474 moraines and rock avalanches in the Upper Romanche valley (French Alps): Evidence of
475 two glacial advances during the Late Glacial/Holocene transition. *Quaternary Science*
476 *Reviews* 148, 209-221.

477 Clark, P.U., Dyke, A.S., Shakun, J.D., Carlson, A.E., Clark, J., Wohlfarth, B., Mitrovica,
478 J.X., Hostetler, S.W., & McCabe, A.M. 2009: The Last Glacial Maximum. *Science* 325,
479 710-714.

480 Clark, C. D., Hughes, A. L. C., Greenwood, S. L., Jordan, C. & Sejrup, H. P. 2012: Pattern
481 and timing of retreat of the last British-Irish Ice Sheet. *Quaternary Science Reviews* 44,
482 112–146.

483 Coquin, J., Mercier D., Bourgeois, O., Cossart, E., & Decaulne, A. 2015: Gravitational
484 spreading of mountain ridges coeval with Late Weichselian deglaciation: impact on glacial
485 landscapes in Tröllaskagi, northern Iceland. *Quaternary Science Reviews* 107, 197-213.

486 Cossart, E., Mercier, D., Decaulne, A., Feuillet, T., Jónsson, H.P., & Sæmundsson, Þ. 2014:
487 Impacts of post-glacial rebound on landslide spatial distribution at a regional scale in
488 northern Iceland (Skagafjörður). *Earth Surface Processes and Landforms* 39, 336-350.

489 CRONUS-Earth Project (<http://web1.itc.ku.edu:8888/html/latest/topo/>) (accessed in
490 August 2015).

491 Decaulne, A., Cossart, E., Mercier, D., Feuillet, T., Coquin, J., & Jónsson, H.P. 2016: An
492 early Holocene age for the Vatn landslide (Skagafjörður, central northern Iceland): Insights
493 into the role of postglacial landsliding on slope development. *The Holocene* 26, 1304-1318.

494 Dede, V., Cicek, I., Sarikaya, M.A., Ciner, A., & Uncu, L. 2017: First cosmogenic
495 geochronology from the Lesser Caucasus: Late Pleistocene glaciation and rock glacier
496 development in the Karçal Valley, NE Turkey. *Quaternary Science Reviews* 164, 54-67.

- 497 Desilets, D., Zreda, M., Almasi, P.F., & Elmore, D. 2006: Determination of cosmogenic Cl-
498 36 in rocks by isotope dilution: innovations, validation and error propagation. *Chemical*
499 *Geology* 233, 185-195.
- 500 Dunai, T.J. 2010: *Cosmogenic Nuclides: Principles, Concepts and Applications in the*
501 *Earth Surface Sciences*. Cambridge University Press, Cambridge.
- 502 Einarsson, Th. 1967: Zu der Ausdehnung der weichselzeitlichen vereisung Nordislands.
503 *Sonderveröffentlichungen des Geologischen Institutes der Universität Köln* 13, 167-173.
- 504 Einarsson, Th. 1973: Geology of Iceland. In Pitcher, M.G. (ed.) *Arctic geology*. American
505 Association of Petroleum Geologists Memoir 19, 171-175.
- 506 Eiríksson, J., Knudsen, K. L. Hafliðason, H. & Henriksen, P. 2000: Late-glacial and
507 Holocene palaeoceanography of the North Iceland Shelf. *Journal of Quaternary Science*
508 15, 23-42.
- 509 Eddudóttir, S.D., Erlendsson, E., & Gísladóttir, G. 2015: Life on the periphery is tough:
510 Vegetation in Northwest Iceland and its responses to early-Holocene warmth and later
511 climate fluctuations. *The Holocene* 25, 1437-1453.
- 512 Eddudóttir, S.D., Erlendsson, E., Tinganelli, L., & Gísladóttir, G. 2016: Climate change
513 and human impact in a sensitive ecosystem: the Holocene environment of the Northwest
514 Icelandic highland margin. *Boreas* 54, 715-728.
- 515 Feuillet, T., Coquin, J., Mercier, D., Cossart, E., Decaulne, A., Jónsson, H.P., &
516 Sæmundsson, Þ. 2014: Focusing on the spatial non-stationarity of landslide predisposing
517 factors in northern Iceland: do paraglacial factors vary over space? *Progress Physical*
518 *Geography* 38, 354-377.
- 519 Fink, D., Vogt, S., & Hotchkis, M. 2000: Cross-sections for ³⁶Cl from Ti at Ep = 35–150
520 MeV: applications to in-situ exposure dating. *Nuclear Instruments and Methods in Physics*
521 *Research Section B: Beam Interactions with Materials and Atoms* 172, 861–866.
- 522 Geirsdóttir, Á., Andrews, J.T., Ólafsdóttir, S., Helgadóttir G., & Harðardóttir J. 2002: A 36
523 Ky record of iceberg rafting and sedimentation from north-west Iceland. *Polar Research*
524 21, 291-298.
- 525 Geirsdóttir, A., Miller, G.H., Axford, Y., & Ólafsdóttir, S. 2009: Holocene and latest
526 Pleistocene climate and glacier fluctuations in Iceland. *Quaternary Science Reviews* 28,
527 2107–2118.
- 528 Geirsdóttir, A., Miller, G.H., Larsen, D.J., & Ólafsdóttir, S. 2013: Abrupt Holocene climate
529 transitions in the northern North Atlantic region recorded by synchronized lacustrine
530 records in Iceland. *Quaternary Science Reviews* 70, 48-62.
- 531 Gil, I., Keigwin, L.D. & Abrantes, F. 2015: The deglaciation over Laurentian Fan: History
532 of diatoms, IRD, ice and fresh water. *Quaternary Science Reviews* 129, 57-67.
- 533 Harning, D.J., Geirsdóttir, Á., Miller, G.H., & Zalzal, K. 2016: Early Holocene deglaciation
534 of Drangajökull, Vestfirðir, Iceland. *Quaternary Science Reviews* 153, 192-198.
- 535 Hjartarson, Á. & Sæmundsson, K. 2014: *Geological Map of Iceland*, 1:600.000, Bedrock.
536 ÍSOR, Icelandic Geosurvey, Reykjavík.

- 537 Hubbard, A., Sugden, J. Dugmore, A., Norðdahl H., & Pétursson H. G. 2006: A modelling
538 insight into the Icelandic Late Glacial Maximum ice sheet. *Quaternary Science Reviews* 25,
539 2283-2296.
- 540 Hughes, A. L., Gyllencreutz, R., Lohne, Ø. S., Mangerud, J., & Svendsen, J. I. 2016: The
541 last Eurasian ice sheets-a chronological database and time - slice reconstruction, DATED
542 - 1. *Boreas*, 45(1), 1-45.
- 543 Icelandic Meteorological Office, 2018. *Climatological data*. Available
544 <http://en.vedur.is/climatology/data/> (accessed 13 April 2018).
- 545 Ingólfsson, Ó. & Norðdahl, H. 2001: High Relative Sea Level during the Bølling
546 Interstadial in Western Iceland: A Reflection of Ice-sheet Collapse and Extremely Rapid
547 Glacial Unloading. *Arctic, Antarctic, and Alpine Research* 33, 231-243.
- 548 Ingólfsson, Ó., Björck, S., Hafliðason H., & Rundgren M. 1997: Glacial and climatic
549 events in Iceland reflecting regional North Atlantic climatic shifts during the Pleistocene-
550 Holocene transition. *Quaternary Science Reviews*. 16, 1135-1144.
- 551 Ivy-Ochs, S. 2015. Glacier variations in the European Alps at the end of the last glaciation.
552 *Cuadernos de Investigación Geográfica* 41, 45-65.
- 553 Ivy-Ochs, S., Synal, H.A., Roth, C., & Schaller, M. 2004: Initial results from isotope
554 dilution for Cl and Cl-36 measurements at the PSI/ETH Zurich AMS facility. *Nuclear*
555 *Instruments and Methods in Physics Research Section B: Beam Interactions with Materials*
556 *and Atoms* 223-224, 623-627.
- 557 Jaccard, S.L., Galbraith, E.D., Martínez-García, A., & Anderson R.F. 2016: Covariation of
558 deep Southern Ocean oxygenation and atmospheric CO₂ through the last ice age. *Nature*,
559 530, 207–210.
- 560 Jónsson, Ó. 1976: *Berghlaup. Ræktunarfélag Norðurlands*. 623 pp. Akureyri.
- 561 Kaldal, I. & Víkingsson, S. 1990: Early Holocene deglaciation in Central Iceland. *Jökull*
562 40, 51-66.
- 563 Kleman, J. & Applegate, P.J. 2014: Durations and propagation patterns of ice sheet
564 instability events. *Quaternary Science Reviews* 92, 32-39.
- 565 Larsen, D., Miller, G.H., Geirsdottir, A., & Olafsdottir, S. 2012: Non-linear Holocene
566 climate evolution in the North Atlantic: a high-resolution, multi-proxy record of glacier
567 activity and environmental change from Hvítárvatn, central Iceland. *Quaternary Science*
568 *Reviews* 39, 14-25.
- 569 Liakka, L., Löfverström, M., & Colleoni, F. 2016: The impact of the North American
570 glacial topography on the evolution of the Eurasian ice sheet over the last glacial cycle.
571 *Climate of the Past* 12, 1225–1241.
- 572 Licciardi, J.M., Denoncourt, C.L., & Finkel, R.C. 2008: Cosmogenic ³⁶Cl production rates
573 from Ca spallation in Iceland. *Earth and Planetary Science Letters* 267, 365-377.
- 574 Lippold, J., Gutjahr, M., Blaser, P., Christner, E., Carvalho Ferreira, M.L., Mulitz, C.,
575 Christl, M., Wombacher, F., Böhm, E., Antz, B., Cartapanis, O., Vogel, H., & Jaccard,

576 S.L. 2016: Deep water provenance and dynamics of the (de)glacial Atlantic meridional
577 overturning circulation. *Earth and Planetary Science Letters*, 445, 68–78.

578 Malmberg, S.A. 1985: The water masses between Iceland and Greenland. *Journal of*
579 *Marine Research Institute* 9, 127-140.

580 Marrero, S., Phillips, F.M., Borchers, B., Lifton, N., & Aumer, R. 2016a: Cosmogenic
581 nuclide systematics and the CRONUScal program. *Quaternary Geochronology* 31, 160-
582 187.

583 Marrero, S., Phillips, F.M., Hinz, M., Caffee, M., & Gosse, J. 2016b: CRONUS-Earth
584 cosmogenic ³⁶Cl calibration. *Quaternary Geochronology*. 31, 199-219.

585 McDougall, I., Kristjansson, L. & Sæmundsson, K. 1984: Magnetostratigraphy and
586 geochronology of NW-Iceland. *Journal of Geophysical Research* 89: 7029–7060.

587 McManus, J.F., Francois, R., Gherardi, J.M., Keigwin, L.D., & Brown-Leger, S. 2004:
588 Collapse and rapid resumption of Atlantic meridional circulation linked to deglacial climate
589 changes. *Nature*, 428, 834–837.

590 Mercier, D., Cossart, E., Decaulne, A., Feuillet, T., Jónsson, H.P., & Sæmundsson, Þ.,
591 2013: The Höfðahólar rock avalanche (sturzström): chronological constraint of paraglacial
592 landsliding on an Icelandic hillslope. *The Holocene* 23, 432-446.

593 Mercier, D., Coquin, J., Feuillet, T., Decaulne, A., Cossart, E., Jónsson, H.P., &
594 Sæmundsson, Þ., 2017: Are Icelandic rock-slope failures paraglacial? Age evaluation of
595 seventeen rock-slope failures in the Skagafjörður area, based on geomorphological
596 stacking, radiocarbon dating and tephrochronology. *Geomorphology* 296, 45–58.

597 Moorbath, S., Sigurdson, H. & Goodwin, R. 1968: K-Ar ages of oldest exposed rocks in
598 Iceland. *Earth and Planetary Science Letter* 26 4: 197-205.

599 Norðdahl, H. 1991: A review of the glaciation maximum concept and the deglaciation of
600 Eyjafjörður, North Iceland. In Maizels, J.K. & Caseldine, C. (eds.): *Environmental*
601 *Changes in Iceland: Past and Present*, 31–47, Kluwer Academic Publishers, Dordrecht.

602 Norðdahl, H., Haflidason, H., 1992. The Skógar tephra, a Younger Dryas marker in North
603 Iceland. *Boreas* 21, 23–41.

604 Norðdahl, H. & Einarsson Th. 2001: Concurrent changes of relative sea-level and glacier
605 extent at the Weichselian – Holocene boundary in Berufjörður, Eastern Iceland. *Quaternary*
606 *Science Reviews* 20, 1607-1622.

607 Norðdahl, H. & Pétursson H. G. 2005: Relative sea level changes in Iceland. New aspects
608 of the Weichselian deglaciation of Iceland. In Caseldine, C., Russel, A., Harðardóttir, J., &
609 Knudsen, Ó. (eds.): *Iceland - Modern Processes and Past Environments*, 25-78, Elsevier,
610 Amsterdam.

611 Norðdahl, H., Ingólfsson, Ó., Pétursson H. G., & Hallsdóttir M. 2008: Late Weichselian
612 and Holocene environmental history of Iceland. *Jökull* 58, 343-364.

613 Norðdahl, H., & Ingólfsson, Ó. 2015: Collapse of the Icelandic ice sheet controlled by sea-
614 level rise? *Arktos* 1(1), 13.

- 615 Palacios, D., Andrés, N., Gómez Ortiz, A., & García-Ruiz, J.M. 2017a: Evidence of glacial
616 activity during the Oldest Dryas in the mountains of Spain. *In* Hughes P. D. & Woodward,
617 J. C. (eds.): *Quaternary Glaciation in the Mediterranean Mountains*. 87-110. Geological
618 Society, London.
- 619 Palacios, D., García-Ruiz, J.M., Andrés, N., Schimmelpfennig, I., Campos, N. Leanni, L.,
620 & ASTER Team. 2017b: Deglaciation in the central Pyrenees during the Pleistocene-
621 Holocene transition: Timing and geomorphological significance. *Quaternary Science*
622 *Reviews* 162, 111-127.
- 623 Patton, H., Hubbard, A., Bradwell, T. & Schomacker, A. 2017: The configuration,
624 sensitivity and rapid retreat of the Late Weichselian Icelandic ice sheet. *Earth-Science*
625 *Reviews* 166. 223–245.
- 626 Pétursson, H.G., Norðdahl, H., & Ingólfsson, O. 2015: Late Weichselian history of relative
627 sea level changes in Iceland during a collapse and subsequent retreat of marine based ice
628 sheet. *Cuadernos de Investigación Geográfica* 41, 261-277.
- 629 Phillips, F.M. 2003: Cosmogenic ^{36}Cl ages of Quaternary basalt flows in the Mojave
630 Desert, California, USA. *Geomorphology* 53, 199-208.
- 631 Principato, S.M., Geirsdottir, A., Johannsdottir, G.E., & Andrews, J.T. 2006: Late
632 Quaternary glacial and deglacial history of eastern Vestfirðir. *Journal of Quaternary*
633 *Sciences* 21, 271–285.
- 634 Renssen, H., Seppä, H., Crosta, X., Goosse, H., & Roche, D.M. 2012: Global
635 characterization of the Holocene thermal maximum. *Quaternary Science Reviews* 48, 7-19.
- 636 Rundgren, M. 1995: Biostratigraphic evidence of the Allerød -Younger Dryas-Preboreal
637 oscillation in Northern Iceland. *Quaternary Research*, 44, 405-416.
- 638 Rundgren, M. 1999: A summary of the environmental history of the Skagi peninsula,
639 northern Iceland, 11,300-7800 BP. *Jökull* 47, 1-19.
- 640 Rundgren, M. & Ingólfsson, Ó. 1999: Plant survival in Iceland during periods of
641 glaciations. *Journal of Biogeography* 26, 387-396.
- 642 Schimmelpfennig, I. 2009: *Cosmogenic ^{36}Cl in Ca and K rich minerals: analytical*
643 *developments, production rate calibrations and cross calibration with ^3He and ^{21}Ne* . 324
644 pp. PhD These Université Paul Cézanne Aix-Marseille III, CEREGE, Aix en Provence,
645 France.
- 646 Schimmelpfennig, I., Benedetti, L., Finkel, R., Pik, R., Blard, P.H., Bourlès, D., Burnard,
647 P., & Williams, A. 2009: Sources of *in situ* ^{36}Cl in basaltic rocks. Implications for
648 calibration of production rates. *Quaternary Geochronology* 4, 441–461.
- 649 Schimmelpfennig, I., Benedetti, L., Garreta, V., Pik, R., Blard, P.H., Burnard, P., Bourlès,
650 D., Finkel, R., Ammon, K., & Dunai, T. 2011: Calibration of cosmogenic ^{36}Cl production
651 rates from Ca and K spallation in lava flows from Mt. Etna (38°N, Italy) and Payun Matru
652 (36°S, Argentina). *Geochimica et Cosmochimica Acta* 75, 2611-2632.
- 653 Schimmelpfennig, I., Schaefer, J.M., Putnam, A.E., Koffman, T., Benedetti, L., Ivy-Ochs,
654 S., Aster Team, & Schulüchter, Ch. 2014: ^{36}Cl production rate from K-spallation in the

- 655 European Alps (Chironico landslide, Switzerland). *Journal of Quaternary Science* 29, 407-
656 413.
- 657 Schomacker, A., Brynjólfsson, S., Andreassen, J.M., Gudmundsdóttir, E.R., Olsen, J.,
658 Odgaard, B.V., Hákkansson, L., Ingólfsson, Ó. & Larsen, N.K. 2016: The Drangajökull
659 ice cap, northwest Iceland, persisted into the early-mid Holocene. *Quaternary Science*
660 *Reviews* 148, 68-84.
- 661 Sigurðsson, O. & Williams, R.S. 2008: *Geographic names of Iceland's Glaciers: historic*
662 *and modern*. 225 pp. U.S. Geological Survey Professional Paper 1746. U.S. Geological
663 Survey, Reston, Virginia.
- 664 Sinclair, G., Carlson, A.E., Mix, A.C., Lecavalier, B.S., Milne, G., Mathias A., Buizert. C.,
665 & DeConto, R. 2016: Diachronous retreat of the Greenland ice sheet during the last
666 deglaciation. *Quaternary Science Reviews* 145, 243-258.
- 667 Spagnolo, M. & Clark, C.D. 2009: A geomorphological overview of glacial landforms on
668 the Icelandic continental shelf. *Journal of Maps* 5, 37-52.
- 669 Stokes, C. R. 2017: Deglaciation of the Laurentide Ice Sheet from the Last Glacial
670 Maximum. *Cuadernos de Investigación Geográfica* 43, 377-428.
- 671 Stokes, C.R., Corner, G.D., Winsborrow, M.C.M., Husum, K., & Andreassen, K. 2014:
672 Asynchronous response of marine-terminating outlet glaciers during deglaciation of the
673 Fennoscandian Ice Sheet. *Geology* 42, 455-458.
- 674 Stokes, C. R. and twenty five authors more, 2015: On the reconstruction of palaeo-ice
675 sheets: Recent advances and future challenges, *Quaternary Science Reviews* 125, 15-49.
- 676 Stone, J.O. 2000: Air pressure and cosmogenic isotope production. *Journal of Geophysical*
677 *Research* 105, 23753-23759.
- 678 Stone, J.O., Allan, G.L., Fifield, L.K., & Cresswell, R.G. 1996: Cosmogenic ^{36}Cl from
679 calcium spallation. *Geochimica et Cosmochimica Acta* 60, 679-692.
- 680 Stone, J.O., Fifield, K., & Vasconcelos, P. 2005: *Terrestrial chlorine-36 production from*
681 *spallation of iron*. Abstract of 10th International Conference on Accelerator Mass
682 Spectrometry. September 5-10, 2005, Berkeley, USA.
- 683 Striberger, J., Björck, S., Holmgren, S., & Hamerlík, L. 2012: The sediments of Lake
684 Lögurinn - A unique proxy record of Holocene glacial meltwater variability in eastern
685 Iceland. *Quaternary Science Reviews* 38, 76-88.
- 686 Stroeven, A.P., Hättstrand, C., Kleman, J., Heyman, J., Fabel, D., Fredin, O., Goodfellow,
687 B.W., Harbor, J.M., Jansen, J.D., Olsen, L., Caffee, M.W., Fink, D., Lundqvist, J.,
688 Rosqvist, G.C., Strömberg, B., & Jansson, K.N. 2016: Deglaciation of Fennoscandia.
689 *Quaternary Science Reviews* 147, 91-121
- 690 Stötter, J., Wastl, M., Caseldine, C. & Häberle, T. 1999: Holocene palaeoclimatic
691 reconstructions in Northern Iceland: approaches and results. *Quaternary Science Reviews*
692 18, 457-474.

693 Swanson, T.W. & Caffee, M.L. 2001: Determination of ^{36}Cl production rates derived from
694 the well-dated deglaciation surfaces of Whidbey and Fidalgo Islands, Washington.
695 *Quaternary Research* 56, 366-382.

696 Sæmundsson, K. 1979: Outline of the geology of Iceland. *Jökull*, 29, 7-28.

697 Sæmundsson, K., Kristjánsson, L., McDougal, I. & Warkins, N.D. 1980: K-Ar dating,
698 geological and paleomagnetic study of a 5-km lava succession in Northern Iceland. *Journal*
699 *of Geophysical Research*, 85, 3628-3646.

700 Vasskog K., Langebroek, P.M., Andrews, J.T., Nilsen, J.E.Ø., & Nesje, A. 2015: The
701 Greenland Ice Sheet during the last glacial cycle: Current ice loss and contribution to sea-
702 level rise from a palaeoclimatic perspective. *Earth-Science Reviews* 150, 45–67.

703 Víkingsson, S. 1978: The deglaciation of the southern part of the Skagafjörður district,
704 northern Iceland. *Jökull*, 28, 1-17.

705 Wangensteen B., Guðmundsson Á., Eiken T., Käab A., Farbrót H., & Etzelmüller B. 2006:
706 Surface displacements and surface age estimates for creeping slope landforms in Northern
707 and Eastern Iceland using digital photogrammetry. *Geomorphology* 80, 59–79

708 Wastl, M., Stötter, J., & Caseldine, C. 2001: Reconstruction of Holocene variations of the
709 upper limit of tree or shrub birch growth in northern Iceland based on evidence from
710 Vesturardalur-Skiðadalur, Trollaskagi. *Arctic, Antarctic and Alpine Research* 33, 191-203.

711 Watkins, N.D. and Walker, G.P.L. 1977: Magnetostratigraphy of eastern-Iceland. *American*
712 *Journal of Science*, 277: 513–584.

713 Wirsig, C., Zasadni, J., Christl, M., Akçar, N., & Ivy-Ochs, S. 2016: Dating the onset of
714 LGM ice surface lowering in the High Alps. *Quaternary Science Reviews* 143, 37–50.

715 Zreda, M., Enbglund, J., Phillips, F., Elmore, D., & Sharma, P. 1999: Unblocking of the
716 Nares Strait by Greenland and Ellesmere ice-sheet retreat 10,000 years ago. *Nature* 398,
717 128-142.

718 Xiao, X., Zhao, M., Knudsen, K.L., Sha, L., Eiríkssone, J. Guðmundsdóttire, E., Jiang, H.,
719 & Guo, Z. 2017: Deglacial and Holocene sea–ice variability north of Iceland and response
720 to ocean circulation changes. *Earth and Planetary Science Letters* 472, 14–24.

721

722 **Tables**

723 Table 1. Geographical locations of samples, topographical shielding factor and sample thickness of ^{36}Cl samples from Skagafjörður
 724 (northern Iceland).

Location	Sample ID	Sample type	Distance from the Hofsjökull snout (km)	Latitude °N (DD)	Longitude °W (DD)	Elevation (m a.s.l.)	Topographic shielding factor (unitless)	Thickness (cm)
Skagafjörður and Highlands	IF-2	Erratic boulder	26	65.1568	18.6599	704	0.91	2.0
	IF-3	Polished bedrock	36	65.1984	18.8703	645	1.00	4.0
	IF-4	Polished bedrock	69	65.4413	19.3074	148	0.98	4.0
	IF-5	Polished bedrock	70	65.4418	19.3075	152	0.97	4.0
	IF-6	Polished bedrock	89	65.5979	19.3332	122	0.97	2.5
	IF-7	Polished bedrock	92	65.6209	19.3479	139	1.00	3.0
	IF-8	Polished bedrock	104	65.7164	19.4914	129	1.00	2.5
	IF-9	Polished bedrock	135	65.9603	19.4862	138	0.98	2.5
	Skagi peninsula	SK-1	Polished bedrock	132	65.9047	19.8990	162	0.98
SK-2		Polished bedrock	146	65.9971	19.9819	137	0.98	2.0
SK-3		Polished bedrock	161	66.0969	20.2680	95	0.95	4.0
Eyjafjörður	AKU-1	Polished bedrock	96	65.6448	18.1101	202	0.93	2.0
	AKU-2	Polished bedrock	124	65.8988	18.3137	210	0.87	5.0

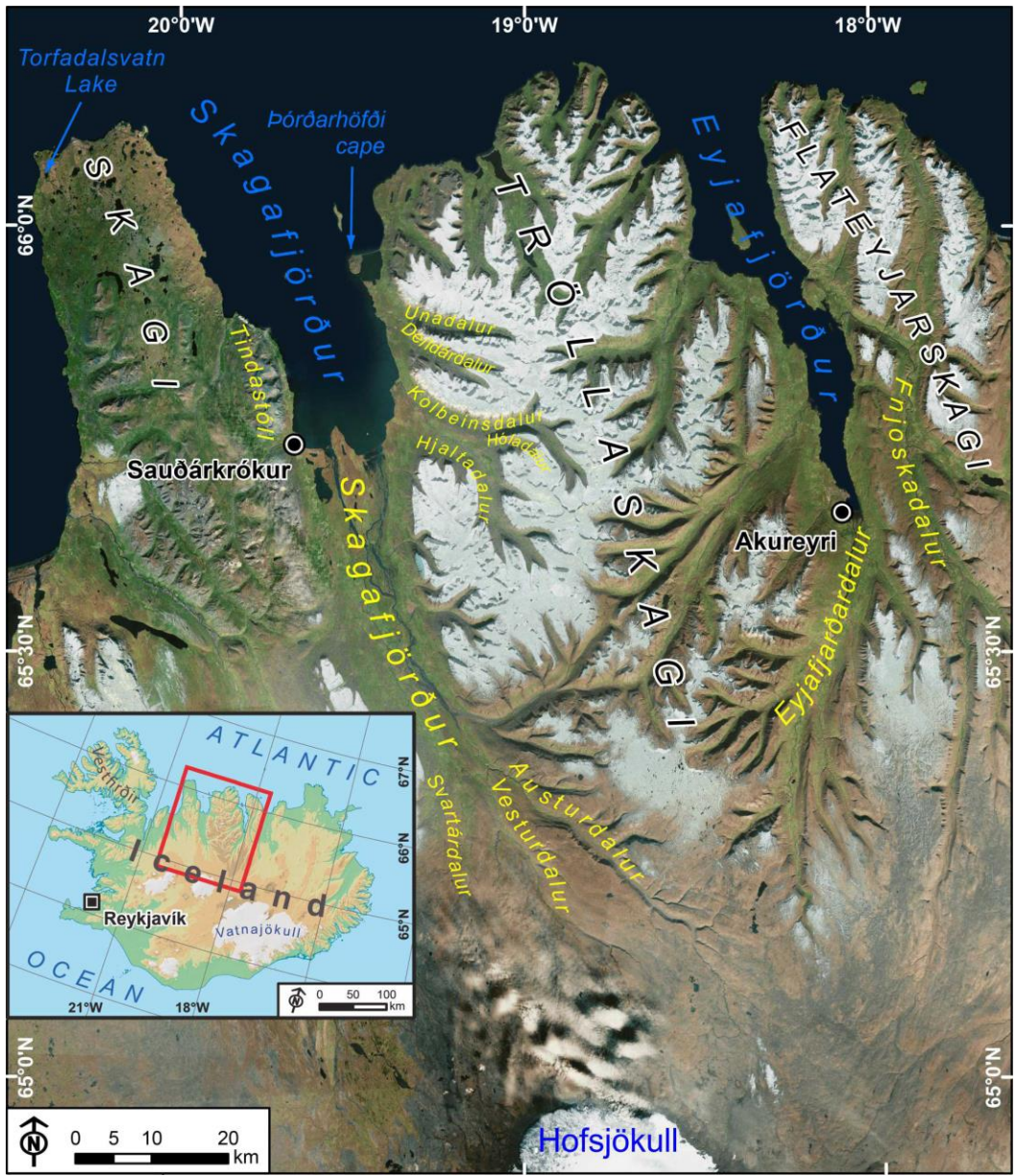
725

726 Table 2. ^{36}Cl exposure ages from Skagafjörður (northern Iceland). Spike enriched in ^{35}Cl (99.66%). Dilution spike $^{35}\text{Cl}/^{37}\text{Cl}$ ratio is
 727 293.8 ± 3.1 . Ages are reported for 0 mm/ka erosion rate. Two age uncertainties are reported: the first figure shows analytical
 728 uncertainties only and the second (in parentheses) includes analytical uncertainties and production rate errors (one standard deviation).
 729 (*) Scaled total sample specific ^{36}Cl production rate without radiogenic (including ^{36}Cl production rate by spallation of Ca, K, Fe, and

730 Ti; by capture of epithermal neutrons; by capture of thermal neutrons; and by capture of slow negative muons). (1) Data calculated
731 from ^{36}Cl production rate from Ca spallation = 48.8 ± 3.4 atoms ^{36}Cl (g Ca) $^{-1}$ yr $^{-1}$ from Stone *et al.* (1996) and scaling factors
732 calculated with local atmospheric pressure (Stone 2000). (2) Data calculated from ^{36}Cl production rate from Ca spallation s = $57.3 \pm$
733 5.2 atoms ^{36}Cl (g Ca) $^{-1}$ yr $^{-1}$ from Licciardi *et al.* (2008) and scaling factors calculated with no atmospheric pressure correction (Stone
734 2000). Analytical data of ^{36}Cl samples from Skagafjörður are provided in Table S1

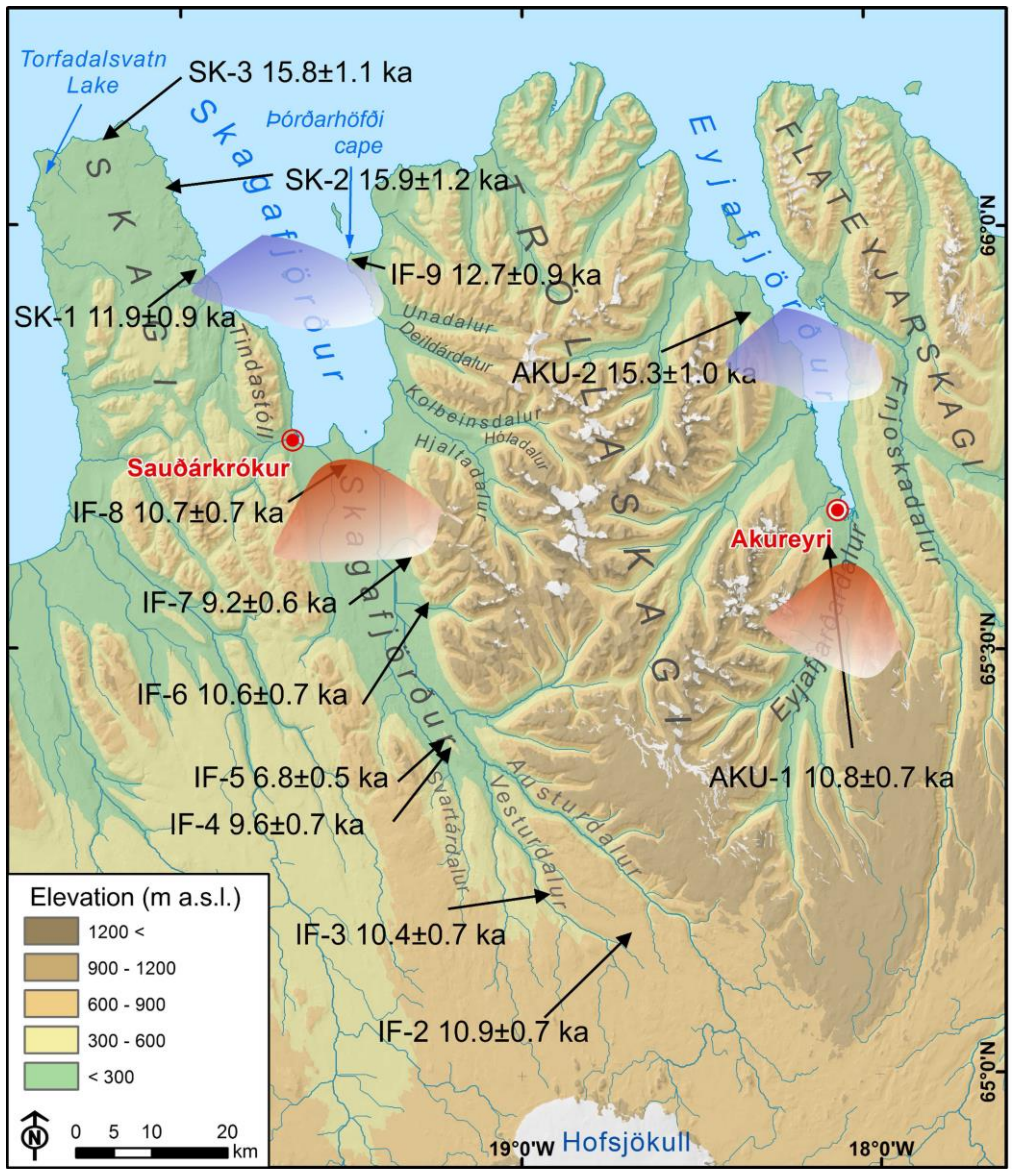
Location	Sample ID	Sample mass (g)	Mass of ^{35}Cl spike solution (mg)	Analytical stable isotope ratio ($^{35}\text{Cl}/(^{35}\text{Cl}+^{37}\text{Cl})$)	Analytical $^{36}\text{Cl}/\text{Cl}$ ratio ($^{36}\text{Cl}/10^{15}\text{Cl}$)	Measured ^{36}Cl concentration (10^4 atoms ^{36}Cl g $^{-1}$)	^{36}Cl Production rate (*)		Age calculated with spallation production rate for Ca = 48.8 ± 3.4 atoms ^{36}Cl (g Ca) $^{-1}$ yr $^{-1}$ (Stone <i>et al.</i> , 1996) (ka)	Age calculated with spallation production rate for Ca = 57.3 ± 5.2 atoms ^{36}Cl (g Ca) $^{-1}$ yr $^{-1}$ (Licciardi <i>et al.</i> , 2008) (ka)
							(1)	(2)		
Skagafjörður fjord and Highlands	IF-2	30.54	1.0084	6.67 ± 0.0350	101.29 ± 3.49	12.3 ± 0.4	11.3	11.7	10.9 ± 0.7 (1.0)	10.6 ± 0.7 (1.0)
	IF-3	30.69	1.0102	7.57 ± 0.0490	107.88 ± 3.72	11.6 ± 0.4	11.3	11.7	10.4 ± 0.7 (0.9)	10.0 ± 0.7 (1.0)
	IF-4	30.10	0.9960	13.20 ± 0.0910	85.81 ± 3.35	6.8 ± 0.3	7.1	7.5	9.6 ± 0.7 (0.9)	9.1 ± 0.6 (0.9)
	IF-5	30.45	0.9906	14.23 ± 0.2180	63.46 ± 2.22	4.8 ± 0.2	7.1	7.5	6.8 ± 0.5 (0.6)	6.5 ± 0.4 (0.6)
	IF-6	31.30	1.0031	27.78 ± 0.2180	108.54 ± 4.28	6.9 ± 0.3	6.6	7.1	10.6 ± 0.7 (1.0)	9.9 ± 0.7 (1.0)
	IF-7	30.19	0.9807	19.55 ± 0.0770	95.73 ± 3.31	6.6 ± 0.2	7.3	7.8	9.2 ± 0.6 (0.8)	8.6 ± 0.6 (0.9)
	IF-8	30.28	1.0096	10.31 ± 0.0890	74.94 ± 2.60	6.7 ± 0.2	6.3	6.6	10.7 ± 0.7 (0.9)	10.2 ± 0.7 (1.0)
	IF-9	31.11	0.9953	5.19 ± 0.0200	63.30 ± 2.64	10.3 ± 0.4	8.0	8.3	12.7 ± 0.9 (1.3)	12.4 ± 0.9 (1.3)
	Skagi peninsula	SK-1	30.14	0.9974	26.61 ± 0.1740	113.21 ± 5.86	7.5 ± 0.4	6.3	6.8	11.9 ± 0.9 (1.2)
SK-2		30.01	0.9635	6.57 ± 0.0630	92.52 ± 4.60	11.1 ± 0.6	7.0	7.3	15.9 ± 1.2 (1.5)	15.2 ± 1.2 (1.6)
SK-3		30.09	1.0350	9.87 ± 0.0870	98.62 ± 3.75	9.3 ± 0.4	5.9	6.2	15.8 ± 1.1 (1.4)	15.0 ± 1.0 (1.5)
Eyjafjörður fjord	AKU-1	30.40	0.9296	8.22 ± 0.0320	83.17 ± 2.88	7.8 ± 0.3	7.3	7.7	10.8 ± 0.7 (1.0)	10.3 ± 0.7 (1.0)
	AKU-2	30.50	0.9548	17.15 ± 0.1250	133.46 ± 4.36	9.2 ± 0.3	6.1	6.5	15.3 ± 1.0 (1.4)	14.4 ± 1.0 (1.4)

735



736

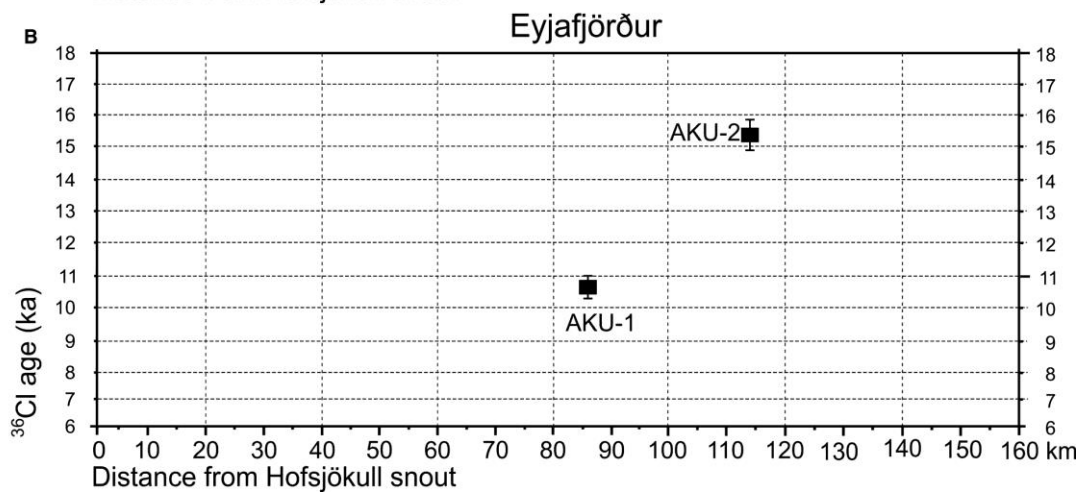
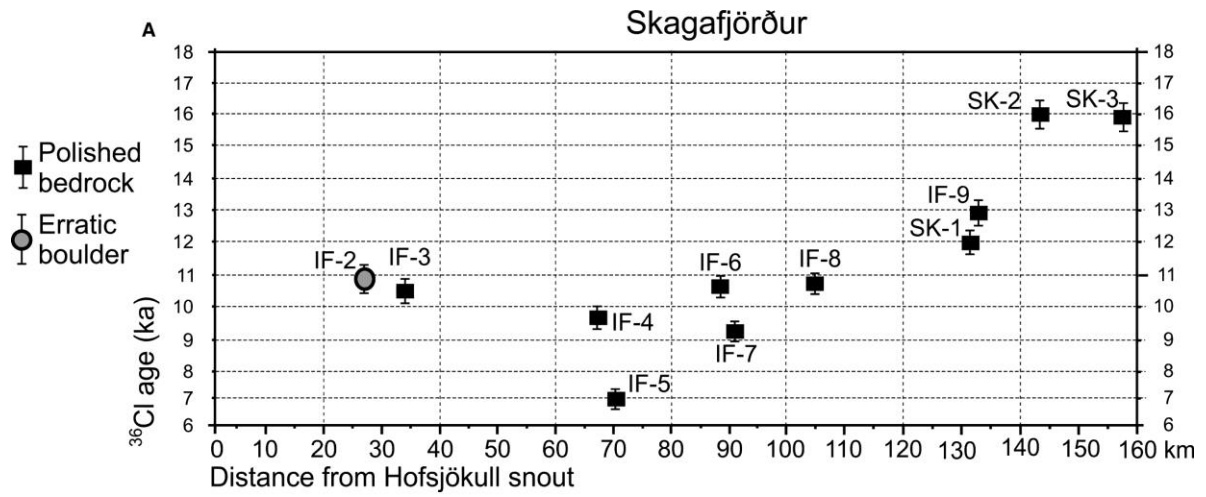
737



Limits of the glacier during Younger Dryas Limits of the glacier during Pre-Boreal

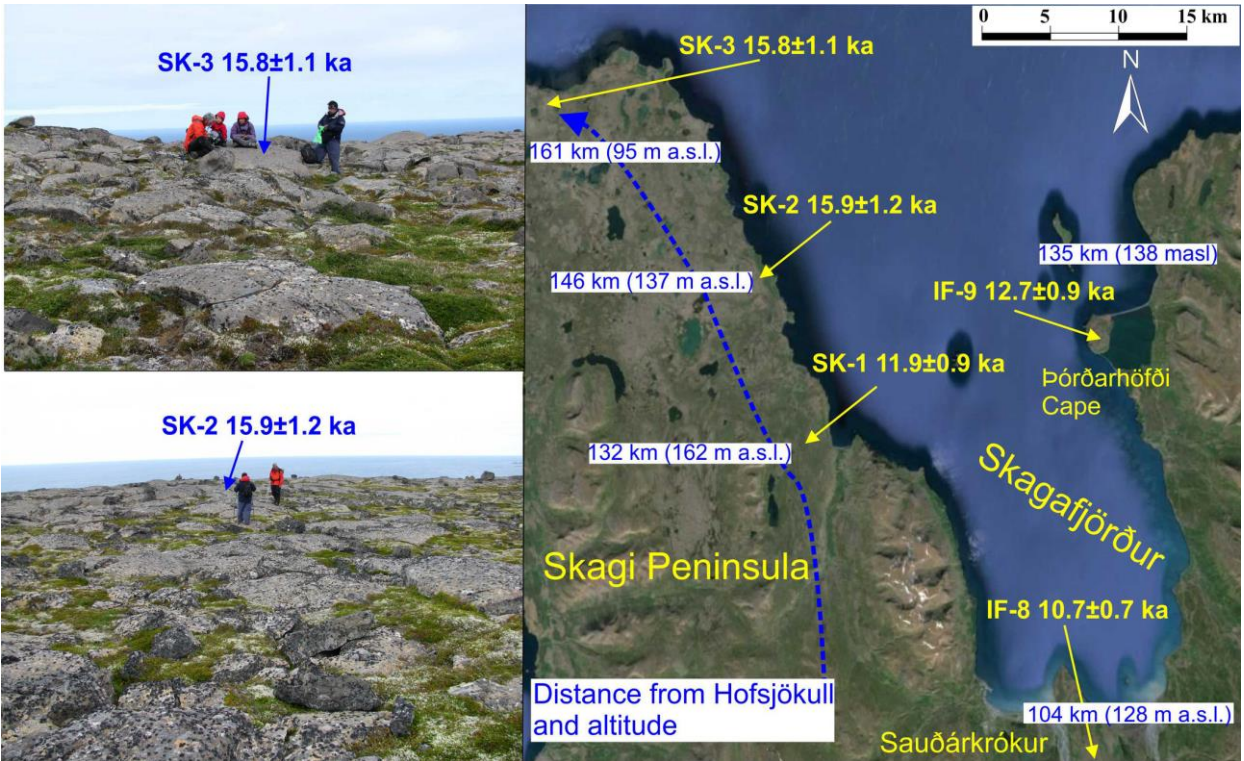
738  Pétursson et al. (2015)  Pétursson et al. (2015)

739



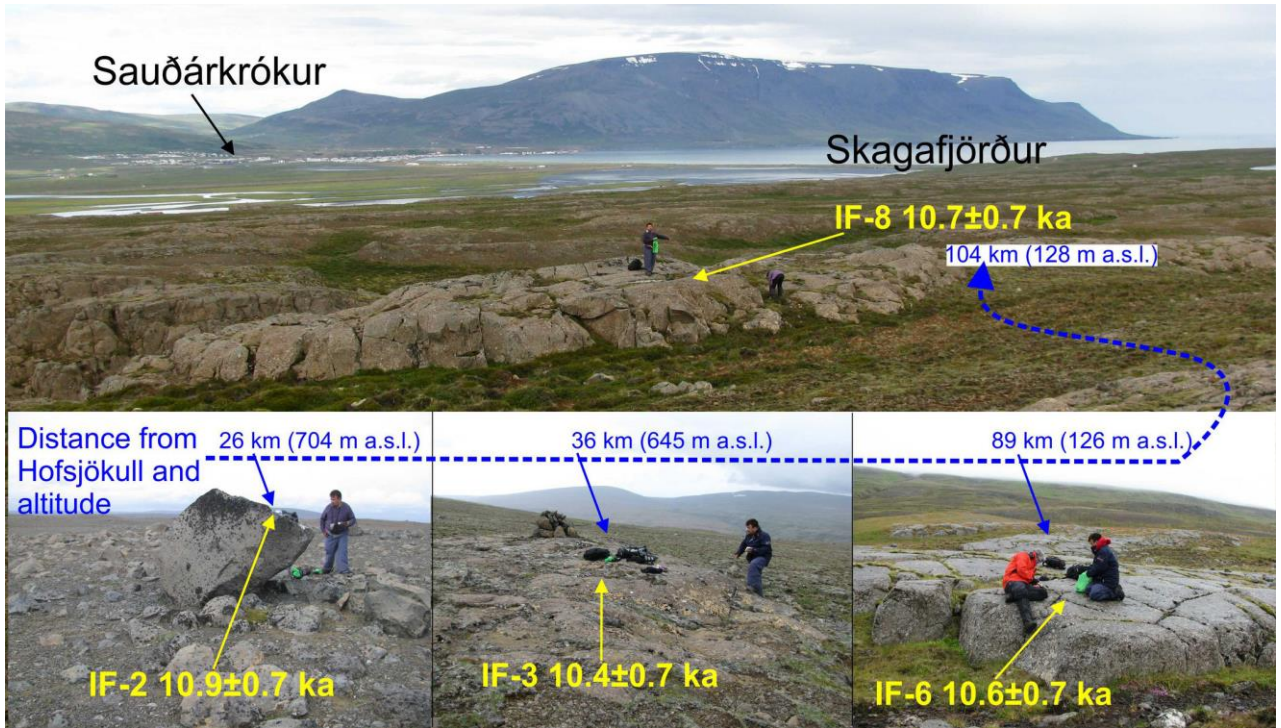
740

741



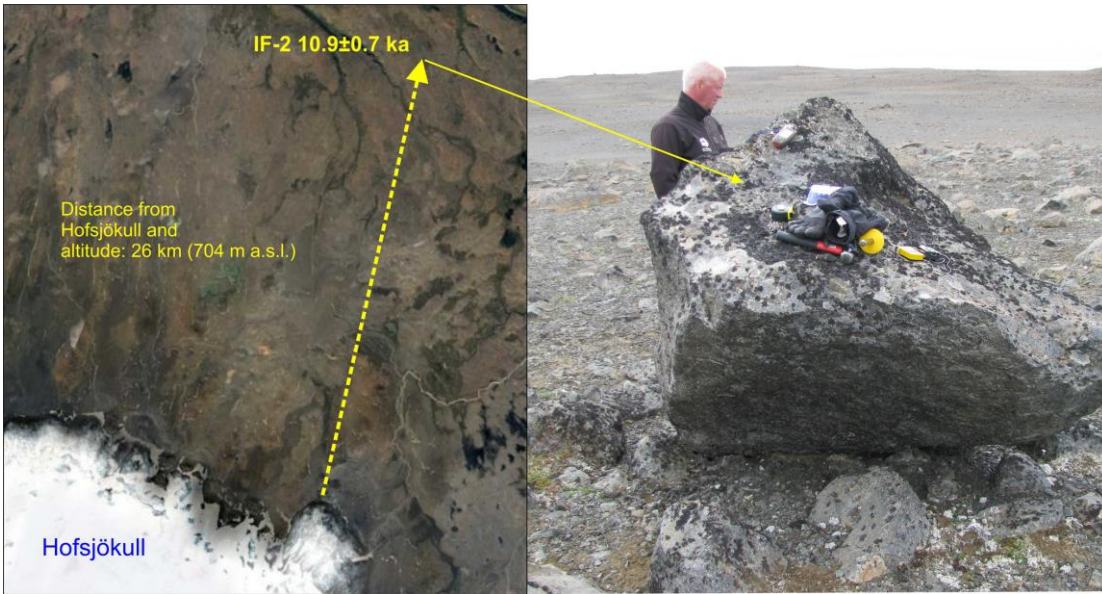
742

743



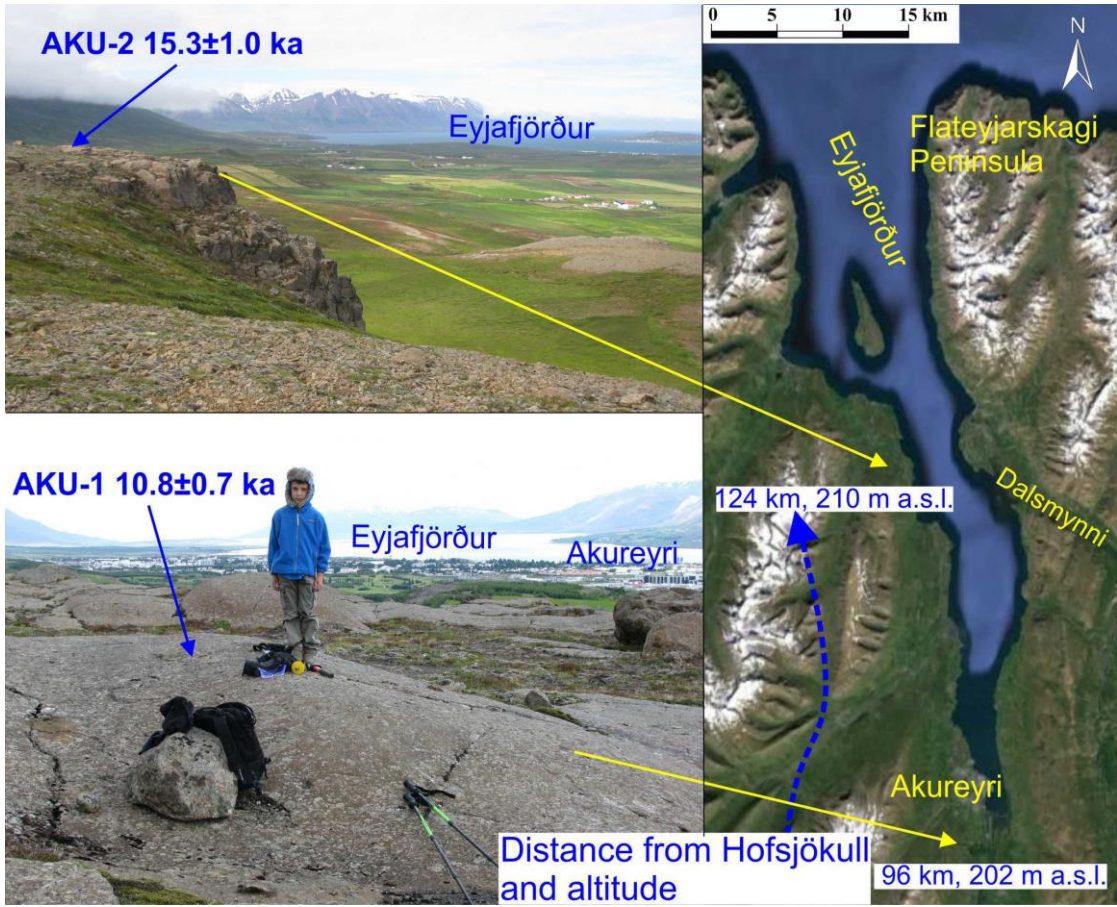
744

745



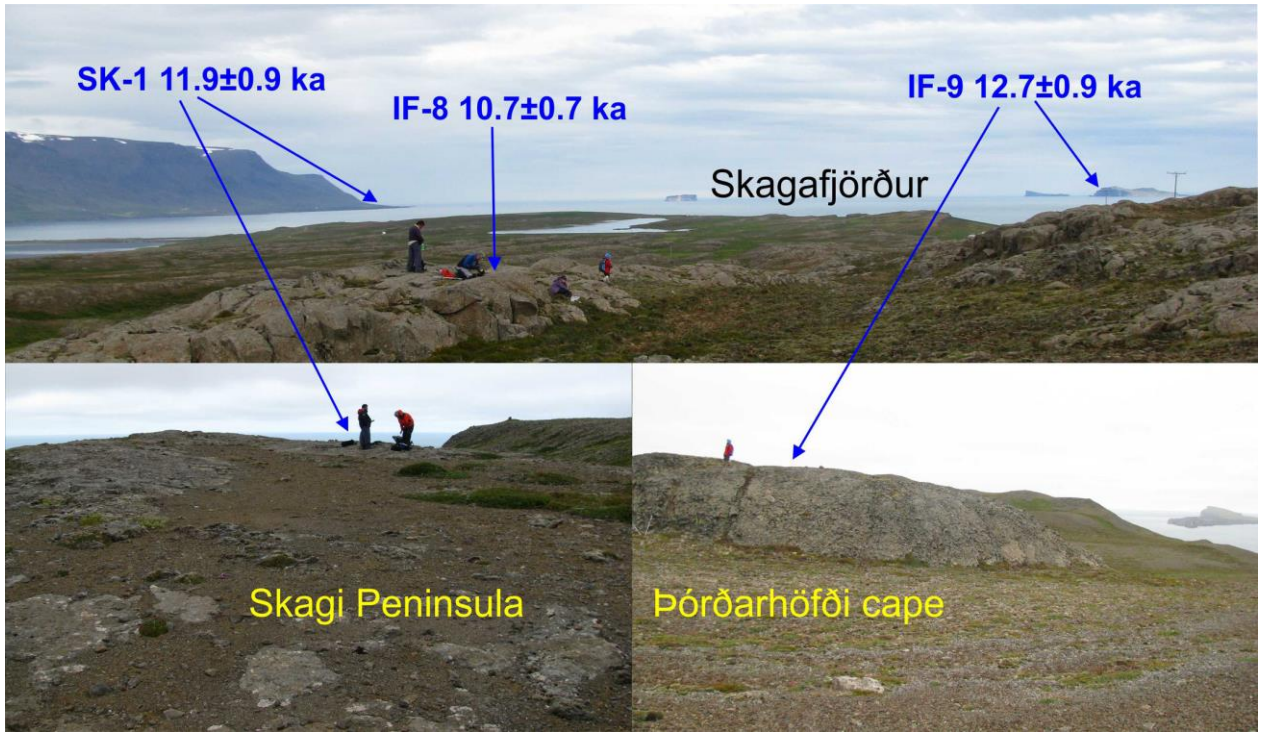
746

747



748

749



750

751

752 **FIGURE CAPTIONS**

753 Figure 1. Location of the study area, villages, main valleys, peninsulas and fjords cited in
754 the text. See detailed map in Figure 2.

755

756 Figure 2. Location of sampling sites and ice margins at different ages, according to
757 previous deglaciation models (Pétursson *et al.* 2015).

758

759 Figure 3. Cosmogenic exposure dates and their distribution in relation to distance from the
760 northern margin of the Hofsjökull ice cap.

761

762 Figure 4. Erratic boulder located 26 km north of the northern margin of the Hofsjökull ice
763 cap at 704 m a.s.l. (for location see Fig. 2).

764

765 Figure 5. Polished surfaces and erratic boulder at various sites sampled within the
766 Skagafjörður (for location see Fig. 2).

767

768 Figure 6. Polished surfaces at the present coastline in Skagafjörður, close to Sauðarkrókur
769 village and from the Skagi peninsula to the west and the Þórðarhöfði semi-island to the east
770 (for location see Fig. 2).

771

772 Figure 7. Polished surfaces on the Skagi peninsula (for location see Fig. 2).

773

774 Figure 8. Polished surfaces at the Eyjafjörður, and CRE samples taken from the head and
775 middle of the fjord.

776

777 **Supporting information**

778

779 Table S1. Analytical data for ^{36}Cl samples from Skagafjörður (Northern Iceland).